

# Quantum quench and non-equilibrium dynamics in lattice-confined spinor condensates

Z. Chen, T. Tang, J. Austin, Z. Shaw, L. Zhao, and Y. Liu\*

*Department of Physics, Oklahoma State University, Stillwater, Oklahoma 74078, USA*

(Dated: May 22, 2019)

We present an experimental study on non-equilibrium dynamics of a spinor condensate after it is quenched across a superfluid to Mott insulator (MI) phase transition in cubic lattices. Intricate dynamics consisting of spin-mixing oscillations at multiple frequencies are observed in time evolutions of the spinor condensate localized in deep lattices after the quantum quench. Similar spin dynamics also appear after spinor gases in the MI phase are suddenly moved away from their ground states via quenching magnetic fields. We confirm these observed spectra of spin-mixing dynamics can be utilized to reveal atom number distributions of an inhomogeneous system, and to study transitions from two-body to many-body dynamics. Our data also imply the non-equilibrium dynamics depend weakly on the quench speed but strongly on the lattice potential. This enables precise measurements of the spin-dependent interaction, a key parameter determining the spinor physics.

A spinor Bose-Einstein condensate (BEC) is a multi-component condensate possessing a spin degree of freedom [1]. Combined with optical lattices and microwave dressing fields, spinor gases offer an unprecedented degree of control over many parameters and have thus been considered as ideal candidates for studying complicated non-equilibrium dynamics [1–12]. Such a spinor system can be easily prepared far away from equilibrium through quenching one of its highly-controllable parameters, e.g., the number of atoms, temperature, total spin of the system, the lattice potential, or the dimensionality of the system [1–10]. Interesting dynamics have also been initiated in lattice-confined spinor gases by non-equilibrium initial states, such as interaction-driven revival dynamics in one-dimensional Ising spin chains [13], dynamics and equilibration of spinor BECs in two-dimensional lattices [3], and spin-mixing dynamics of tightly confined atom pairs in cubic lattices [14, 15]. Another notable advantage of spinor systems on investigating non-equilibrium dynamics is their long equilibration time, ranging from tens of milliseconds to several seconds [1, 3]. Experimental studies on non-equilibrium dynamics have been conducted in spinor gases extensively at two extremes, i.e., in a clean two-body system with a pair of atoms in the Mott-insulator (MI) phase [14, 15], and in a many-body system with more than  $10^4$  atoms in the superfluid (SF) phase [1–4]. Transitions between these two extremes, however, remain less explored [5].

In this paper, we experimentally confirm that lattice-trapped spinor BECs provide a perfect platform to understand these less-explored transitions. Our experiments are performed in a quantum quench scenario starting with an antiferromagnetic spinor BEC at its SF ground state, based on a theoretical proposal in Ref. [5]. We continuously quench up the potential of a cubic lattice to a very large value, which completely suppresses tunnellings to freeze out atom number distributions in individual lattice sites. Rich spin dynamics are observed at fast quench speeds and adiabatic SF-MI quantum phase transitions are detected after sufficiently slow lattice ramps. About

half of the data shown in this paper are collected after the lattice is quenched at an intermediate speed, which is slow enough to prevent excitations to higher vibrational bands while remaining fast enough to suppress hopping among lattice sites. We observe intricate dynamics consisting of spin-mixing oscillations at multiple frequencies in spinor BECs after the quantum quench in magnetic fields of strength  $B < 60 \mu\text{T}$ . The rest of our data are taken after adiabatic lattice ramps. Similar spin dynamics also occur after we abruptly move spinor gases in the MI phase away from their ground states via quenching magnetic fields. In our system, an inhomogeneous system with an adjustable peak occupation number per lattice site ( $n_{\text{peak}}$ ), a significant amount of lattice sites are occupied by more than two atoms. The observed spin-mixing spectra are thus utilized to study transitions between two-body and many-body spin dynamics and to reveal atom number distributions of an inhomogeneous system. Our data also indicate the non-equilibrium dynamics depend weakly on the quench speed but strongly on the lattice potential. Every observed spin dynamics is found to be well described by a sum of multiple Rabi-type spin-mixing oscillations. This enables us to precisely measure the ratio of the spin-independent interaction  $U_0$  to the spin-dependent interaction  $U_2$ , an important factor determining the spinor physics.

The site-independent Bose-Hubbard model has successfully described lattice-confined spinor BECs [5, 16, 17]. We can thus understand our data taken in deep lattices with a simplified Bose-Hubbard model by ignoring the tunnelling energy  $J$  as follows [5, 17],

$$H = \frac{U_0}{2}n(n-1) + \frac{U_2}{2}(\vec{S}^2 - 2n) + q(n_1 + n_{-1}) - \mu n. \quad (1)$$

Here  $U_2$  is positive (negative) in antiferromagnetic (ferromagnetic) spinor BECs,  $q$  is the net quadratic Zeeman energy induced by magnetic and microwave fields,  $\mu$  is the chemical potential,  $n = \sum_{m_F} n_{m_F}$  is the total atom number in each lattice site with  $n_{m_F}$  atoms staying in the hyperfine  $m_F$  state, and  $\vec{S}$  is the spin operator [5, 17].

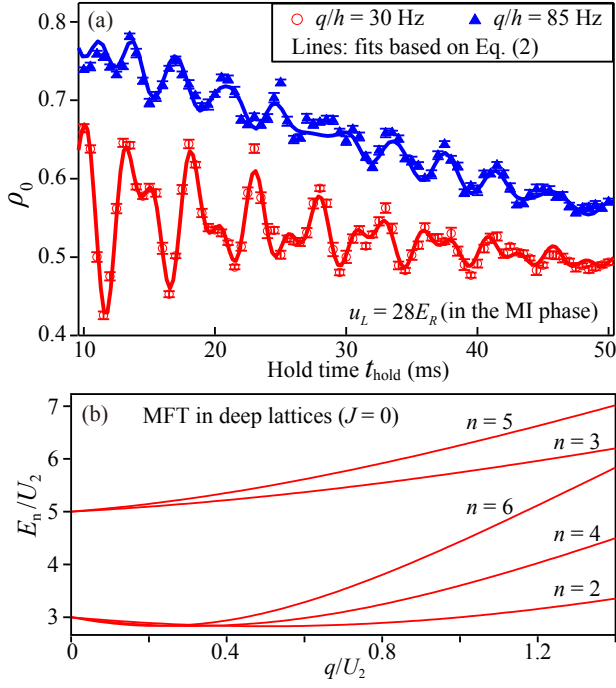


FIG. 1. (a) Observed dynamics of spin-0 atoms after Quench-Q sequences to different  $q$ . Lines are fits based on Eq. (2). (b) Lines denote the predicted energy  $E_n = h \cdot f_n$  (see text).

In our experiment, we start each cycle at  $q/h = 40$  Hz in free space with a spin-1 antiferromagnetic spinor BEC of up to  $10^5$  sodium ( $^{23}\text{Na}$ ) atoms in its ground state, the longitudinal polar (LP) state with  $\rho_0 = 1$  and  $m = 0$  [18]. Here  $\rho_{m_F}$  is the fractional population of the  $m_F$  state,  $m = \rho_{+1} - \rho_{-1}$  is the magnetization, and  $h$  is the Lank constant. Two different quench sequences, Quench-L and Quench-Q, are applied in this paper. In the Quench-L sequences, we tune magnetic fields to a desired  $q$  and then quench up the depth  $u_L$  of a cubic lattice from 0 to  $28E_R$  within a time duration  $t_{\text{ramp}}$ , where  $E_R$  is the recoil energy [18]. This final depth  $u_L$  is much larger than SF-MI transition points and thus deep enough to localize atoms into individual lattice sites. We carefully set  $t_{\text{ramp}}$  based on two criteria (see Ref. [19]). In the Quench-Q sequences, we adiabatically ramp up cubic lattices to a final depth of  $u_L \geq 28E_R$  in a high field (where  $q \gg U_2$ ), which ensures atoms cross SF-MI transitions and enter into their ground states (where  $\rho_0 \simeq 1$ ) in the MI phase [16]; and we then suddenly quench magnetic fields to a desired  $q$  for initiating non-equilibrium dynamics. After each quench sequence, atoms are held in lattices for a certain time  $t_{\text{hold}}$  followed by being abruptly released from the lattices and detected via the microwave imaging.

Interesting non-equilibrium dynamics consisting of spin-mixing oscillations at multiple frequencies are observed after both Quench-L and Quench-Q sequences in spinor gases localized in deep lattices at  $q/h < 100$  Hz. Two typical time evolutions detected after Quench-Q se-

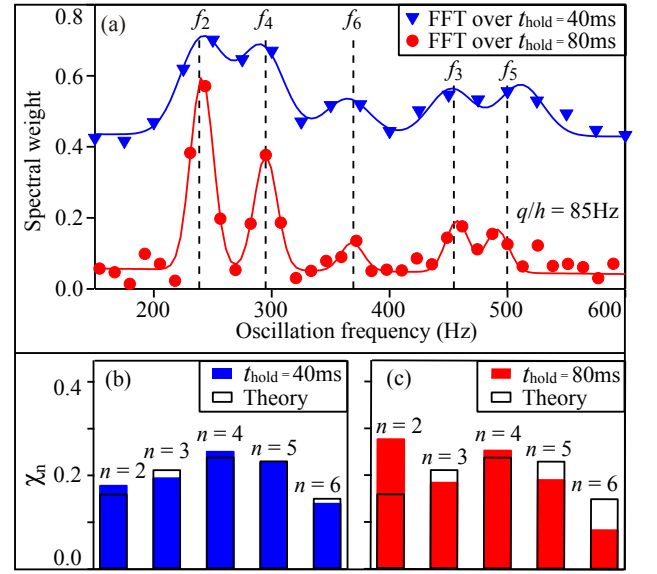


FIG. 2. (a) Triangles (circles) represent fast Fourier transformations (FFT) over the first 40 ms (80 ms) of  $t_{\text{hold}}$  on the  $q/h = 85$  Hz data set shown in Fig. 1 (a). Vertical lines mark the predicted  $f_n$  (see text). Solid lines are five-Gaussian fits. Results obtained at  $t_{\text{hold}} = 40$  ms are shifted up by 0.4 for visual clarity. (b) Atom number distributions extracted from the  $t_{\text{hold}} = 40$  ms FFT spectrum in Panel (a). We define  $\chi_n$  as the fraction of atoms localized in lattice sites having  $n$  atoms, and extract  $\chi_n$  from dividing the area below the corresponding peak in a FFT spectrum by the spin oscillation amplitude  $D_n$  (see Ref. [20]). Black bars mark the predicted  $\chi_n$  in Mott-insulator shells at  $n_{\text{peak}} = 6$  based on Eq. (1) and the Thomas-Fermi approximation. (c) Similar to Panel (b) but extracted from the  $t_{\text{hold}} = 80$  ms FFT spectrum in Panel (a).

quences are shown in Fig. 1(a). Such an evolution appears to be fit by a composition of multiple Rabi-type oscillations (see solid lines in Fig. 1(a) and Eq. (2)). This can be explained by considering that  $n$  atoms tightly confined in one lattice site display a Rabi-type oscillation at a fixed frequency  $f_n$ , and the observed dynamics combine all time evolutions occurring in individual lattice sites for our inhomogeneous system. We derive  $f_n = E_n/h$  from the mean-field theory (MFT), where  $E_n$  is the energy gap between the ground state and the first excited state at a given  $n$  (see Fig. 1(b)). Analytical expressions for  $f_n$  can be found at  $n = 2$  and  $n = 3$ , i.e.,  $f_2 = U_2 \sqrt{9 - 4(q/U_2) + 4(q/U_2)^2}/h$  and  $f_3 = U_2 \sqrt{25 + 4(q/U_2) + 4(q/U_2)^2}/h$ . We develop the following empirical formula based on the predicted  $f_n$  for an inhomogeneous system with a certain  $n_{\text{peak}}$ , and find all observed spin dynamics can be fit by this formula (see typical examples in Fig. 1(a)),

$$\rho_0(t) = \sum_{n=2}^{n_{\text{peak}}} A_n \exp(-t/\tau_n) \sin[2\pi f_n(t - t_0)] + \Delta\rho_0 \exp(-t/\tau_0) + \frac{1}{3}. \quad (2)$$

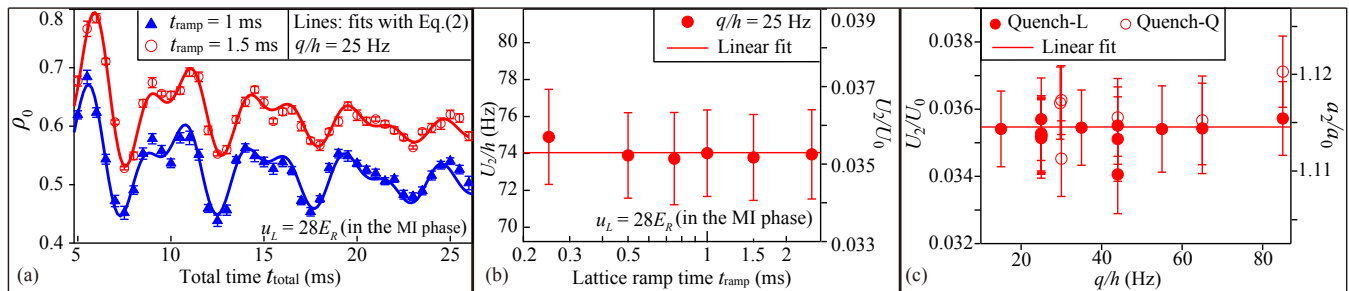


FIG. 3. (a) Observed spin dynamics after Quench-L sequences at two  $t_{\text{ramp}}$ . Lines are fits based on Eq. (2). Data taken at  $t_{\text{ramp}} = 1.5$  ms are shifted up by 0.1 for visual clarity. (b) Extracted  $U_2$  and  $U_2/U_0$  from fitting observed dynamics with Eq. (2) at various  $t_{\text{ramp}}$ . The horizontal line is a linear fit. (c) Similar to Panel (b) but extracted from our data taken under 20 different conditions. The right axis marks the corresponding ratio  $a_2/a_0 = (U_2 + U_0)/(U_0 - 2U_2)$ , where  $a_0$  and  $a_2$  are scattering lengths.

Here the first term combines individual Rabi-type oscillations at all possible  $n$  with  $1/\tau_n$  being the damp rate for oscillation amplitudes and  $t_0$  marking the beginning of oscillations, while the second term describes an overall decay of spin oscillations at a decay rate of  $1/\tau_0$ . This decay may be mainly due to unavoidable lattice-induced heatings. The third term of Eq. (2) is based on Refs. [3, 21] and indicates the three spin components equally distribute in equilibrium states when  $t_{\text{hold}} \rightarrow \infty$ .

To better illustrate the spin-mixing dynamics, we conduct fast Fourier transformations (FFT) onto all observed time evolutions. Two typical FFT spectra extracted from the same data set over different time durations are shown in Fig. 2(a), where the vertical lines mark the five  $f_n$  predicted by MFT. Each of these two FFT spectra has five distinguished peaks agreeing well with the MFT predictions, i.e., all spin components in the three even Mott lobes oscillate at lower frequencies while particles in the two odd Mott lobes display higher spin oscillation frequencies when  $q/U_2 < 1.55$ . Atom number distributions in the spinor gases can also be revealed from the corresponding FFT spectrum over a given time duration, as explained in Figs. 2(b) and 2(c). A comparison between these two figures clearly demonstrates that number distributions  $\chi_n$  in our system quickly change with time  $t_{\text{hold}}$  and the  $n = 2$  Mott lobe becomes more dominating after atoms are held in deep lattices for a longer time. This implies atoms in the  $n = 2$  Mott lobe decay more slowly, which may be owing to a lack of three-body inelastic collisions in this lobe. Figure 2(b) shows another notable result: each experimental  $\chi_n$  extracted from the FFT spectrum over a short time duration (i.e.,  $t_{\text{hold}} = 40$  ms) coincides with the theoretical  $\chi_n$  derived from Eq. (1) and the Thomas-Fermi approximation for Mott-insulator shells at  $n_{\text{peak}} = 6$ . Atoms in initial states distribute into these predicted Mott shells during the Quench-Q sequences, because the initial states are the ground states of the MI phase. Our data thus experimentally confirm that the spin-mixing dynamics and their corresponding FFT spectra over a short  $t_{\text{hold}}$  can

efficiently probe the initial Fock-state distributions after a sufficiently fast quench.

Similar non-equilibrium dynamics composed of various spin-mixing oscillations are also detected in time evolutions of spinor gases after Quench-L sequences under a wide range of magnetic fields, as shown in Fig. 3. To our knowledge, this may be the first experimental observation of such complicated spin-mixing dynamics, although its theoretical model has been studied by Ref. [5]. Our observations indicate the spin-mixing dynamics weakly depend on  $t_{\text{ramp}}$  [22]. Typical examples can be seen in Fig. 3(a), where the data sets collected at distinct  $t_{\text{ramp}}$  display similar dynamics with almost identical oscillation frequencies and slightly different oscillation amplitudes. This may be due to the fact that  $t_{\text{ramp}}$  in a Quench-Q sequence is carefully chosen for limiting all spin components to oscillate between the ground states and the first excited states.

The spin oscillations observed after Quench-L sequences can also be well fit by Eq. (2) (see Fig. 3(a)). We can thus extract the spin-dependent interaction  $U_2$  from these fitting curves, because the oscillation frequencies  $f_n$  are decided by  $U_2$  when  $n \geq 2$  at a fixed  $q$ . Figures 3(b) and 3(c) show 20 experimental values of  $U_2$  extracted from our data taken under very different conditions. By applying linear fits to these data points, we find a precise value for two key parameters that determine the spinor physics, i.e.,  $U_2/U_0 \simeq 0.035(3)$  and  $a_2/a_0 \simeq 1.115(10)$  for  $^{23}\text{Na}$  atoms. Here  $a_2$  and  $a_0$  are s-wave scattering lengths, and  $a_2/a_0 = (U_2 + U_0)/(U_0 - 2U_2)$  based on Ref. [24, 25]. Many published values of  $U_2/U_0$  were derived from the scattering lengths [5, 26–32]. For example, Refs. [26, 27] respectively found scattering lengths that would lead to  $U_2/U_0 = 0.032(14)$  and  $0.035(11)$ . In addition, experimental measurements of the scattering lengths through Feshbach spectroscopy could yield  $U_2/U_0 = 0.037(6)$  [28] and  $0.036(3)$  [29]. Therefore, the observed spin dynamics can conveniently measure spin-dependent interactions and  $U_2/U_0$  with a good resolution.

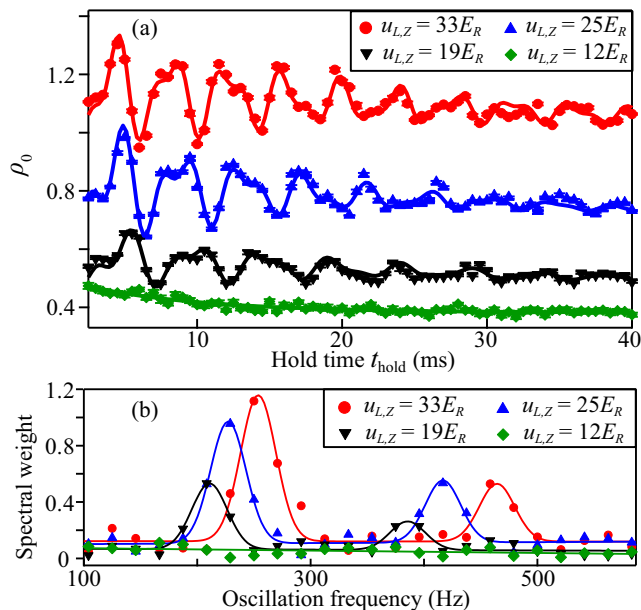


FIG. 4. (a) Observed spin dynamics after Quench-Q sequences to  $q/h = 30$  Hz at various  $u_{L,z}$  while  $u_{L,x} = u_{L,y} = 33E_R$  (see text). Results obtained at  $u_{L,z} = 33E_R, 25E_R,$  and  $19E_R$  are respectively shifted up by 0.55, 0.25, and 0.06 for visual clarity. Lines are fits based on Eq. (2). (b) FFT spectra of the dynamics shown in Panel (a). Lines are two-Gaussian fits.

We also notice one puzzling difference between the non-equilibrium dynamics initiated by a Quench-L sequence and those via a Quench-Q sequence: atoms appear to oscillate with a larger amplitude despite having the same frequencies after the Quench-Q sequence, even if spinor gases are prepared into the same final  $u_L$  and  $q$  by these two quench sequences. This amplitude difference may be attributed to the inevitable dephasing and energy dissipations induced by a number of tunnelling processes. Note that atoms are fully localized in individual lattice sites with negligible tunnellings during Quench-Q sequences. In contrast, spinor gases cross SF-MI phase transitions during a Quench-L sequence, tunnellings among adjacent sites thus cannot be ignored during a certain part of this sequence. Other possible reasons for the different oscillation amplitudes may include significant heatings induced by first-order SF-MI phase transitions at a small  $q$  during Quench-L sequences [16], different atom number distributions introduced by the quench sequences [33], and non-adiabatic lattice ramps in Quench-L sequences.

To understand how tunnellings affect the spin-mixing dynamics, we monitor spin oscillations after varying the tunnelling energy  $J$  in a well-controlled way [8]. We first prepare a non-equilibrium initial state with a Quench-Q sequence to  $q/h = 30$  Hz in a very deep cubic lattice of  $u_{L,x} = u_{L,y} = u_{L,z} = 33E_R$  with  $J \simeq 0$ ; and then suddenly increase  $J$  to a desired value by properly reducing

only one lattice depth  $u_{L,z}$ . Here  $u_{L,x}$ ,  $u_{L,y}$ , and  $u_{L,z}$  are depths of the three lattice beams along orthogonal directions, respectively. Interesting results shown in Fig. 4 are collected at four signature  $u_{L,z}$ , gradually spanning from the few-body dynamics for spinor gases tightly localized in deep lattices at  $u_{L,z} = 33E_R$  with  $J \simeq 0$ , to the many-body dynamics for atoms loosely confined in shallow lattices with  $J \gg 0$  at  $u_{L,z} = 12E_R$ . Amplitudes of spin-mixing oscillations appear to quickly decrease as  $u_{L,z}$  is reduced, and completely vanish when  $u_{L,z} < 14E_R$ . We may understand these observations from two simple illustrations. In one scenario, two atoms oscillate at the frequency  $f_2$  in an  $n = 2$  lattice site. The spin oscillation disappears as one of the two atoms tunnels out of the site. In another scenario,  $n > 2$  atoms oscillate in a lattice site at the frequency  $f_n$ . After one atom hopping out of this site, spin oscillations occurring in this site and the adjacent site that accepts the atom should be changed. Many of such tunnelling events could significantly reduce oscillation amplitudes of the observed spin-mixing dynamics. As  $J$  increases with the reduction of  $u_{L,z}$ , the damping is enhanced and eventually stops the spin oscillations. As a numerical example, the predicted time scale corresponding to  $J$  along the  $z$ -direction is around 3 ms at  $u_{L,z} = 12E_R$ , which is comparable to the damp rate of the observed oscillations (see Fig. 4(a)). These results justify our use of deep lattices and subsequent neglecting of  $J$  in Eq. (1).

Figure 4(b) show the FFT spectra extracted from the non-equilibrium dynamics observed at the four  $u_{L,z}$ . Each of these FFT spectra has only two distinguished peaks rather than the predicted five peaks, i.e., the wide peaks at around 250 Hz correspond to the oscillations of even  $n$  atoms and the wide peaks at around 450 Hz to the oscillations of odd  $n$  atoms. One possible reason for this discrepancy is  $t_{\text{hold}}$  needs to be much longer (greater than 160 ms for all even  $n$ ) to reduce the aliasing effect of the spectrum analysis, but  $t_{\text{hold}}$  in our system is limited by lattice heatings and atom losses. The FFT spectra in Fig. 4(b), however, clearly show that a larger  $u_{L,z}$  leads to spin oscillations of higher frequencies. This can be interpreted by the fact that the oscillation frequency  $f_n$  is determined by  $U_2$  and thus also by the effective lattice depth  $u_L = \sqrt[3]{u_{L,x}u_{L,y}u_{L,z}}$ . Our calculations confirm that the effective  $U_2$  gives oscillation frequencies that fall into those broad peaks seen in Fig. 4(b).

In conclusion, we have presented the first experimental study on few-body spin dynamics and transitions between the well-studied two-body and many-body dynamics in antiferromagnetic spinor BECs. Intricate dynamics consisting of spin-mixing oscillations at multiple frequencies have been observed in time evolutions of the spinor condensate localized in deep lattices after two different quantum quench sequences. We have confirmed these observed spectra of spin-mixing dynamics can reveal atom number distributions of an inhomogeneous system and

also enable precise measurements of two key parameters. The lattice quench method is applicable to other spinor systems, although antiferromagnetic spinor BECs may display larger spin oscillation amplitudes than ferromagnetic spinor gases [5].

We thank Eite Tiesinga for insightful discussions. We also thank the National Science Foundation, the Noble Foundation, and the Oklahoma Center for the Advancement of Science and Technology for financial support.

---

\* Electronic address: yingmei.liu@okstate.edu

- [1] D. M. Stamper-Kurn and M. Ueda, *Rev. Mod. Phys.* **85**, 1191 (2013).
- [2] L. Zhao, J. Jiang, T. Tang, M. Webb, and Y. Liu, *Phys. Rev. A* **89**, 023608 (2014).
- [3] L. Zhao, J. Jiang, T. Tang, M. Webb, and Y. Liu, *Phys. Rev. Lett.* **114**, 225302 (2015).
- [4] C. Becker, P. Soltan-Panahi, J. Kronjäger, S. Dörscher, K. Bongs, and K. Sengstock, *New J. Phys.* **12**, 065025 (2010).
- [5] K. W. Mahmud and E. Tiesinga, *Phys. Rev. A* **88**, 023602 (2013).
- [6] C. B. Dağ, S.-T. Wang, and L.-M. Duan, *Phys. Rev. A* **97**, 023603 (2018).
- [7] M. Lewenstein, A. Sanpera, V. Ahufinger, B. Damski, A. Sen(De), and U. Sen, *Adv. Phys.* **56**, 243 (2007).
- [8] J. S. Krauser, J. Heinze, N. Fläschner, S. Götze, O. Jürgensen, D.-S. Lühmann, C. Becker, and K. Sengstock, *Nat. Phys.* **8**, 813 (2012).
- [9] A. de Paz, A. Sharma, A. Chotia, E. Maréchal, J. H. Huckans, P. Pedri, L. Santos, O. Gorceix, L. Vernac, and B. Laburthe-Tolra, *Phys. Rev. Lett.* **111**, 185305 (2013).
- [10] J. Jiang, L. Zhao, M. Webb, and Y. Liu, *Phys. Rev. A* **90**, 023610 (2014).
- [11] J. Simon, W. S. Bakr, R. Ma, M. E. Tai, P. M. Preiss, and M. Greiner, *Nature* **472**, 307 (2011).
- [12] P. Soltan-Panahi, J. Struck, P. Hauke, A. Bick, W. Plenkers, G. Meineke, C. Becker, P. Windpassinger, M. Lewenstein, and K. Sengstock, *Nat. Phys.* **7**, 434 (2011).
- [13] J. Zeiher, J.-Y. Choi, A. Rubio-Abadal, T. Pohl, R. van Bijnen, I. Bloch, and C. Gross, *Phys. Rev. X* **7**, 041063 (2017).
- [14] A. Widera, F. Gerbier, S. Fölling, T. Gericke, O. Mandel, and I. Bloch, *Phys. Rev. Lett.* **95**, 190405 (2005).
- [15] A. Widera, F. Gerbier, S. Fölling, T. Gericke, O. Mandel, and I. Bloch, *New J. Phys.* **8**, 152 (2006).
- [16] J. Jiang, L. Zhao, S.-T. Wang, Z. Chen, T. Tang, L.-M. Duan, and Y. Liu, *Phys. Rev. A* **93**, 063607 (2016), and the references therein.
- [17] L. Zhao, T. Tang, Z. Chen, and Y. Liu, arXiv:1801.00773 (2018).
- [18] We prepare the LP state by eliminating  $|F = 1, m_F = \pm 1\rangle$  atoms with resonant microwave and laser pulses [17]. The setup and calibration of cubic lattices are identical to those illustrated in our previous work [16].
- [19] First,  $t_{\text{ramp}}$  should be long enough to satisfy the interband adiabaticity requirement  $du_L/dt \ll 32\pi E_R^2/h$  [17]. Second,  $t_{\text{ramp}}$  must be short enough to initiate spin-mixing oscillations, while sufficiently long to limit the oscillations between the ground states and the first excited states.
- [20] Our calculations based on Eq. (1) indicate spin oscillation amplitudes  $D_n$  for an inhomogeneous system with  $n_{\text{peak}} = 6$  at  $q/h = 85$  Hz are  $D_1 = 0$ ,  $D_2 = 0.413$ ,  $D_3 = 0.229$ ,  $D_4 = 0.269$ ,  $D_5 = 0.215$ , and  $D_6 = 0.199$ . Because no spin oscillations occur when  $n = 1$ ,  $\chi_n$  shown in Fig. 2 reflect the normlized number distributions after the  $n = 1$  Mott lobe is excluded.
- [21] N. T. Phuc, Y. Kawaguchi, and M. Ueda, *Phys. Rev. A* **84**, 043645 (2011).
- [22] When  $t_{\text{ramp}} < 1$  ms, we find atoms in our system need additional 1 ms to completely lose their phase coherence. The similar phenomenon has also been reported in rubidium systems [23].
- [23] J. Sebby-Strabley, B. L. Brown, M. Anderlini, P. J. Lee, W. D. Phillips, J. V. Porto, and P. R. Johnson, *Phys. Rev. Lett.* **98**, 200405 (2007).
- [24] T. L. Ho, *Phys. Rev. Lett.* **81**, 742 (1998).
- [25] T. Ohmi and K. Machida, *J. Phys. Soc. Jpn.* **67**, 1822 (1998).
- [26] A. Crubellier, O. Dulieu, F. Masnou-Seeuws, M. Elbs, H. Knöckel, and E. Tiemann, *Eur. Phys. J. D* **6**, 211 (1999).
- [27] F. A. van Abeelen and B. J. Verhaar, *Phys. Rev. A* **59**, 578 (1999).
- [28] C. Samuelis, E. Tiesinga, T. Laue, M. Elbs, H. Knöckel, and E. Tiemann, *Phys. Rev. A* **63**, 012710 (2000).
- [29] S. Knoop, T. Schuster, R. Scelle, A. Trautmann, J. Appmeier, M. K. Oberthaler, E. Tiesinga, and E. Tiemann, *Phys. Rev. A* **83**, 042704 (2011).
- [30] K. Fujimoto and M. Tsubota, *Phys. Rev. A* **88**, 063628 (2013).
- [31] J. Lovegrove, M. O. Borgh, and J. Ruostekoski, *Phys. Rev. Lett.* **112**, 075301 (2014).
- [32] S. Yi and H. Pu, *Phys. Rev. Lett.* **97**, 020401 (2006).
- [33] Z. Chen, J. Austin, Z. Shaw, L. Zhao, and Y. Liu (unpublished)